Relationship Between Electrocardiographic Findings and Cardiac Magnetic Resonance Phenotypes in Arrhythmogenic Cardiomyopathy

Manuel De Lazzari, MD, PhD; Alessandro Zorzi, MD, PhD; Alberto Cipriani, MD; Angela Susana, MD; Giulio Mastella, MD; Alessandro Rizzo, MD; Ilaria Rigato, MD, PhD; Barbara Bauce, MD, PhD; Benedetta Giorgi, MD; Carmelo Lacognata, MD; Sabino Iliceto, MD; Domenico Corrado, MD, PhD; Martina Perazzolo Marra, MD, PhD

Background—The new designation of arrhythmogenic cardiomyopathy defines a broader spectrum of disease phenotypes, which include right dominant, biventricular, and left dominant variants. We evaluated the relationship between electrocardiographic findings and contrast-enhanced cardiac magnetic resonance phenotypes in arrhythmogenic cardiomyopathy.

Methods and Results—We studied a consecutive cohort of patients with a definite diagnosis of arrhythmogenic cardiomyopathy, according to 2010 International Task Force criteria, who underwent electrocardiography and contrast-enhanced cardiac magnetic resonance. Both depolarization and repolarization electrocardiographic abnormalities were correlated with the severity of dilatation/dysfunction, either global or regional, of both ventricles and the presence and regional distribution of late gadolinium enhancement. The study population included 79 patients (60% men). There was a statistically significant relationship between the presence and extent of T-wave inversion across a 12-lead ECG and increasing values of median right ventricular (RV) end-diastolic volume ($P<0.001$) and decreasing values of RV ejection fraction ($P<0.001$). The extent of T-wave inversion to lateral leads predicted a more severe RV dilatation rather than a left ventricular involvement because of the leftward displacement of the dilated RV, as evidenced by contrast-enhanced cardiac magnetic resonance. A terminal activation delay of >55 ms in the right precordial leads (V1-V3) was associated with higher RV volume ($P=0.014$) and lower RV ejection fraction ($P=0.053$). Low QRS voltages in limb leads predicted the presence ($P=0.004$) and amount ($P<0.001$) of left ventricular late gadolinium enhancement.

Conclusions—The study results indicated that electrocardiographic abnormalities predict the arrhythmogenic cardiomyopathy phenotype in terms of severity of RV disease and left ventricular involvement, which are among the most important determinants of the disease outcome. (***J Am Heart Assoc***. 2018;7:e009855. DOI: 10.1161/JAHA.118.009855.)

Key Words: cardiac magnetic resonance imaging • cardiomyopathy • electrocardiography • late gadolinium enhancement

Arrhythmogenic cardiomyopathy (ACM) is an inherited heart disease characterized by fibrofatty myocardial replacement, which may act as a substrate for life-threatening ventricular arrhythmias and cause progressive ventricular systolic dysfunction.[1–3] Previously referred to as arrhythmogenic right ventricular (RV) cardiomyopathy because of the predominant involvement of the RV in the originally reported phenotype, the recognition of biventricular and left-dominant disease variants has led, in recent years, to use of the current designation of ACM, which better reflects the broader phenotypic spectrum of the disease.[2–5]

Conventionally, the diagnosis of ACM relies on clinical criteria that encompass electrocardiographic repolarization and depolarization abnormalities, arrhythmic events, morphofunctional ventricular alterations, histopathologic changes, and familial genetic background.[3] A 12-lead ECG is an integral part of the evaluation of affected patients, and depolarization/repolarization abnormalities are commonly observed, with a reported prevalence of up to 85%.[6] The most striking electrocardiographic abnormalities in patients with ACM include T-wave inversion in anterior or anterolateral leads; prolongation of right precordial QRS duration with a delayed S-wave upstroke (terminal activation delay, >55 ms); QRS fragmentation and postexcitation ε waves (ie, small-amplitude potentials occurring at the end of the QRS complex/beginning of the ST segment); and low QRS voltages in limb leads.[3,6] The underlying structural and functional ventricular abnormalities and the clinical and

prognostic meaning of these electrocardiographic abnormalities remain to be defined.

Because of the advances of machine technology and the increased experience in the interpretation of structural, functional, and tissue characterization findings, contrast-enhanced cardiac magnetic resonance (CE-CMR) has become the most accurate technique for imaging ACM.[5,7,8] The increasing use of CE-CMR showed that left ventricular (LV) involvement is much more common and often occurs earlier than initially thought and a sizeable proportion of patients has a LV involvement that parallels (biventricular ACM) or exceeds the severity of RV involvement (left-dominant ACM).[5,8]

The present study was designed to evaluate the relationship between major electrocardiographic repolarization and depolarization abnormalities and structural and functional CE-CMR findings of both ventricles in a consecutive series of patients with ACM. The aim was to assess the value of routine electrocardiography for the prediction of the ACM phenotype, with particular reference to the severity of RV disease and the presence and extent of LV involvement, which are among the most important determinants of the clinical outcome.[9,10]

Methods

Study Population

The data, analytic methods, and study materials will be available to other researchers for purposes of reproducing the results or replicating the procedure on reasonable request. The study included 79 consecutive patients with a diagnosis of ACM, according to the 2010 International Task Force (ITF) criteria,[3] who underwent CE-CMR from July 2006 to March 2016. In patients enrolled before 2010, the diagnosis was established according to the original 1994 ITF criteria and confirmed using the 2010 revised criteria. CE-CMR findings were not considered for diagnosis. The study was approved by an institutional review committee, and the subjects gave informed consent.

Electrocardiographic Evaluation

A standard 12-lead ECG was recorded at the time of CE-CMR study and evaluated using a digital procedure. The electrocardiographic tracing was interpreted by 2 observers (A.Z. and B.B.) who were unaware of clinical data and CE-CMR findings. Ambiguous cases were reviewed by a third expert (D.C.). Standard measurements included heart rate; rhythm; PR interval; QRS axis, voltage, and duration; and ST-segment and T-wave abnormalities. The following specific electrocardiographic parameters were evaluated: (1) postexcitation ε waves, defined as small-amplitude potentials occurring at the end of the QRS complex/beginning of the ST segment; (2) terminal activation duration (TAD), defined as prolongation of the terminal part of the QRS (from the nadir of the S wave to the end of QRS) >55 ms in leads V1 to V3, in the absence of complete right bundle branch block; (3) low (≤0.5-mV) QRS voltages in limb leads, including both negative and positive components; (4) T-wave inversion (TWI) ≥0.1 mV in depth in ≥2 contiguous leads.[11] According to the presence and extent of TWI across the 12 leads, 3 subgroups were defined: (1) absence of TWI in right precordial leads (V1-V3); (2) TWI limited to right precordial leads (V2-V3); and (3) TWI in right precordial leads, which extended to left precordial (V4-V6) or inferior (II, III, or aVF) leads.[3,6,12,13]

Cardiac Magnetic Resonance

Acquisition protocols

CMR was performed on a 1.5-T scanner (Magnetom Avanto; Siemens Healthcare, Germany) using a comprehensive dedicated protocol. All patients underwent detailed CE-CMR; study protocol included postcontrast sequences. Biventricular morphofunctional assessment was performed by a set of steady-state free precession sequence cine loops in sequential short-axis views (slice thickness, 6 mm; gap, 0 mm;

repetition time, 2.5–3.8 ms; echo time, 1.1–1.6 ms; average in-plane resolution, 1.5×2.4 mm; flip angle, 45°–60°; temporal resolution, 40–45 ms) and long-axis views (2-, 3-, and 4-chamber views) of the LV from the semilunar valve plane through the apex. The RV was evaluated with balanced transaxial Steady-state free precession cine images from the outflow tract to the diaphragm, with a 2-chamber view. After IV administration of contrast agent (gadobenate dimeglumine, Multihance; Bracco; 0.2 mmol/kg of body weight), 2-dimensional segmented fast low-angle shot inversion recovery sequences, after 10 minutes, were acquired in the same views of the cine images, covering the entire ventricles (repetition time, 5.4–8.3 ms; echo time, 1.3–3.9 ms; average in-plane spatial resolution, 1.4–1.5×2.2–2.4 mm; 6-mm slice thickness; 2-mm gap; and flip angle, 20°–25°). Inversion times were adjusted to null normal myocardium using a Look-Locker sequence, and images were repeated in 2 separate phase-encoding directions to exclude artefacts.

Ventricular size and systolic function analysis

Global ventricular volumes and systolic function were calculated from the short-axis cine images, excluding papillary muscles from the myocardium, using a computer-aided analysis package (CMR42; Circle International, Calgary, Alberta, Canada). Ventricular volumes were indexed by body surface area. Analysis of RV global and regional wall motion abnormalities (akinesia or dyskinesia) was based on 5 RV segments: inferior wall, anterolateral wall, RV outflow tract, apex, and inflow tract. Analysis of LV global and regional wall motion abnormalities was based on the 17-segment model proposed by the American Heart Association.

Late gadolinium enhancement assessment

The presence and regional distribution of late gadolinium enhancement (LGE) were visually assessed independently by 2 experienced observers (M.D.L. and B.G.) who were blinded to patient clinical data. Ambiguous cases were reviewed by a third expert (M.P.M.). To exclude artefacts, LGE was deemed present if only visible in 2 orthogonal views (short- and long-axis views). Areas of LGE were allocated to the American Heart Association 17-segment model for the LV and to the 5 regions of the RV.

Displacement of RV toward lateral precordium

Assessment of the degree of lateral displacement of the RV apex toward the left axilla was performed according to a previously reported protocol.[14] In brief, in the long-axis 4-chamber view, the cardiac apex angle was calculated as the angle of the interventricular septum with respect to the thoracic midline; the ratio of lateral displacement was calculated as the ratio between the distance from line A (passing through the midpoint of the sternum and thoracic vertebrae) to the cardiac apex along the internal thoracic cage and the distance from the cardiac apex to line B (orthogonal to line A and passing through the left axilla).

Statistical Analysis

Data are expressed as median with 25th to 75th percentiles because normality could not be assumed for any variable. Categorical differences among groups were evaluated by the χ^2 test or the Fisher exact test, as appropriate. Differences among continuous variables were compared using the Mann-Whitney U test or the Kruskal-Wallis test, as appropriate. A 2-tailed probability value of 0.05 was considered statistically significant. The interobserver reliability analysis for electrocardiographic findings and CMR qualitative parameters was measured by Cohen's κ coefficient. All analyses were performed using SPSS 23 (SPSS Inc, Chicago, IL).

Results

Baseline Clinical and Electrocardiographic Characteristics

The study sample included 79 patients (60% men; median age, 33 years), whose baseline clinical and electrocardiographic characteristics are summarized in Table 1. A normal ECG was found in 7 patients (9%), whereas the others had ≥1 repolarization and depolarization abnormalities. In 18 subjects (23%), there were no TWIs in right precordial leads (V1-V3); in 11 subjects (14%), TWIs were confined to V1 to V3; in 50 subjects (63%), TWIs extended to other leads (to the left precordial leads V4-V6 in 16 [20%]; to the inferior leads II, III, and aVF in 8 [10%]; and to both the left precordial and inferior leads in 26 [33%]). Thirteen patients (16%) exhibited postexcitation "ε" waves. After excluding 12 patients with a right bundle branch block pattern, 27 of the remaining 67 patients (40%) had a prolonged TAD (>55 ms). Low QRS voltages in limb leads were observed in 16 patients (20%). The interobserver reliability for TWI assessment and low voltages in limb leads was κ=1 (95% confidence interval [CI], 1.000–1.000; *P*<0.001); for TAD, κ=0.906 (95% CI, 0.802–1.000; *P*<0.001); and for the ε wave, κ=0.816 (95% CI, 0.641–0.990; *P*<0.001).

CMR Findings

Detailed CE-CMR findings are reported in Table 1. At CE-CMR, 61 patients (77%) showed RV dilatation (median RV end-diastolic volume, 109 mL/m²) and 37 (47%) showed RV dysfunction (median RV ejection fraction, 47%), according to the cutoff proposed by the 2010 ITF criteria. A dilated LV was found in 33 subjects (42%), and a reduced LV ejection fraction

Table 1. Clinical Characteristics of the Overall Sample (n=79)

Characteristics	Value
Age, y	33 (20–48)
Male sex	47 (60)
Family history of sudden death	13 (16)
Clinical symptoms	
Chest pain	5 (6)
Palpitations	42 (53)
Syncope	5 (6)
Dyspnea	8 (10)
International Task Force criteria	
2 Major criteria	42 (53)
1 Major and 2 minor criteria	33 (42)
4 Minor criteria	4 (5)
Electrocardiographic characteristics	
Normal ECG	7 (9)
Depolarization abnormalities	
Postexcitation ε wave	13 (16)
Prolonged terminal activation duration (>55 ms)	27/67 (40)
Low (<0.5-mV) QRS voltages in limb leads	16 (20)
Repolarization abnormalities	
No TWI in right precordial leads (V1-V3)	18 (23)
TWI in right precordial leads (V1-V3) only	11 (14)
TWI in right precordial (V1-V3) plus left precordial (V4-V6) or inferior (II, III, and aVF) leads	50 (63)
Cardiac magnetic resonance features	
Functional analysis	
RV EDV, mL/m^2	109 (94–120)
RV EF, %	47 (37–56)
No. of RV segments with WMA	2 (1–4)
RV volume*	
No dilatation	18 (23)
Minor criteria dilatation	19 (24)
Major criteria dilatation	42 (53)
RV systolic function	
RV EF >45%	42 (53)
RV EF >40%–<45%	11 (14)
RV EF <40%	26 (33)
LV EDV, mL/m^2	85 (73–95)
LV EF, %	58 (50–63)
LV dilatation (≥90 mL/m^2)	33 (42)
LV dysfunction (≤50%)	22 (29)

Table 1. Continued

Characteristics	Value
Tissue characterization analysis	
RV LGE	55 (69)
LV LGE	57 (72)

Values are expressed as number/total (percentage) of patients or median (25th–75th percentile). EDV indicates end-diastolic volume; EF, ejection fraction; LGE, late gadolinium enhancement; LV, left ventricular; RV, right ventricular; TWI, T-wave inversion; WMA, wall motion abnormality.
*According to International Task Force criteria, the cutoff values were >100 mL/m^2 (men) and >90 mL/m^2 (women).

was found in 22 subjects (29%). At postcontrast sequences, LGE was found in 71 patients (90%): the RV was involved in 14 patients (18%), the LV was involved in 16 patients (20%), and both ventricles were involved in 41 patients (52%). In all patients with RV LGE, there was an associated regional wall motion impairment with akinesia or dyskinesia. In all patients with LV LGE a nonischemic pattern of distribution was shown, involving the subepicardial/midmural layers and sparing the subendocardium. The interobserver reliability for the LV LGE was κ=0.907 (95% CI, 0.803–1.000; $P<0.001$); and for the RV LGE, κ=0.798 (95% CI, 0.655–0.941; $P<0.001$).

Comparison Between Electrocardiographic and CMR Findings

The relationship between electrocardiographic and CE-CMR findings is summarized in Tables 2 through 5. The presence of postexcitation ε waves did not correlate with RV and LV dilatation/dysfunction or with LGE (Table 2). Patients with a prolonged TAD (>55 ms in V1-V3) had a larger RV end-diastolic volume (116 versus 99 mL/m^2; $P=0.014$) and a

Table 2. Relationship Between Postexcitation ε Wave and CMR Parameters

Parameters	ε Wave		P Value
	No (n=66)	Yes (n=13)	
RV EDV, mL/m^2	108 (94–118)	109 (98–150)	0.315
RV EF, %	49 (37–58)	41 (35–49)	0.226
RV WMA, no. of segments	2 (1–4)	2 (1–4)	0.968
RV LGE	45 (68)	10 (77)	0.744
LV EDV, mL/m^2	86 (73–95)	85 (70–105)	0.802
LV EF, %	59 (51–62)	51 (44–64)	0.228
LV LGE	46 (70)	11 (85)	0.334

Values are expressed as number (percentage) of patients or median (25th–75th percentile). CMR indicates cardiac magnetic resonance; EDV, end-diastolic volume; EF, ejection fraction; LGE, late gadolinium enhancement; LV, left ventricular; RV, right ventricular; WMA, wall motion abnormality.

Table 3. Relationship Between Prolonged (>55 ms) TAD and CMR Parameters

Parameters	TAD >55 ms		P Value
	No (n=40)	Yes (n=27)	
RV EDV, mL/m^2	99 (92–115)	116 (95–133)	0.014
RV EF, %	50 (44–59)	41 (33–56)	0.053
RV WMA, no. of segments	2 (1–3)	3 (1–4)	0.119
RV LGE	25 (63)	19 (70)	0.506
LV EDV, mL/m^2	82 (72–93)	85 (72–100)	0.288
LV EF, %	59 (53–64)	56 (49–61)	0.088
LV LGE	29 (73)	19 (70)	0.850

Values are expressed as number (percentage) of patients or median (25th–75th percentile). Patients with complete right bundle branch block were excluded.[3] CMR indicates cardiac magnetic resonance; EDV, end-diastolic volume; EF, ejection fraction; LGE, late gadolinium enhancement; LV, left ventricular; RV, right ventricular; TAD, terminal activation duration; WMA, wall motion abnormality.

lower RV ejection fraction (41% versus 50%; P=0.053) than those without a prolonged TAD. There was no association between prolonged TAD and LV dimension, function, or LGE (Table 3). The relationship between the presence and extent of right precordial TWI and CMR parameters is shown in Table 4. There was a statistically significant trend toward increasing RV end-diastolic volume (92, 94, and 117 mL/m^2, respectively; P<0.001) and decreasing RV ejection fraction (57%, 49%, and 41%, respectively; P<0.001) among patients with no TWI, with TWI confined to the right precordial leads, and with TWI extending to the left precordial and/or inferior leads (Figure 1). The degree of lateral displacement of the RV apex toward the left axilla was also related to the presence and extent of right precordial TWI (Figure 2). The median number of RV segments showing regional wall motion abnormalities (1, 2, and 3, respectively; P<0.001) and the presence of RV LGE (50%, 46%, and 82%, respectively; P=0.007) correlated with the presence and extent of right precordial TWI. Instead, none of the LV parameters differed among the 3 groups. Two patients had TWI in both inferior leads (L1, L2, and aVF) and lateral precordial leads (V4-V6), but none in right precordial leads (V1-V3). Both patients had a slight dilation and systolic dysfunction of the LV with evidence of LGE; one also showed low QRS voltages in limb leads. The RV was normal in one patient and appeared slightly dilated in the other.

The presence of low QRS voltages in limb leads was associated with the presence of LV LGE (65% versus 100%; P=0.004) but not with RV LGE (68% versus 75%), reaching a high specificity (100%) with a low sensitivity (28%) (Figure 3). Among the 57 of 79 patients with LV LGE, those with low QRS voltages showed a higher median number of affected LV segments (6 [5–9] versus 3 [2–7] ; P<0.001). No other

functional and structural CMR parameters correlated with low QRS voltages (Table 5).

Discussion

A 12-lead ECG is a fundamental part of the evaluation of patients with ACM. Inverted T waves in right precordial leads, delayed S-wave upstroke, ε waves, low-QRS voltages in limb leads, and intraventricular conduction defects are the most striking electrocardiographic abnormalities in patients with ACM with an overt disease phenotype.[1,2,15] Accordingly, this study showed that a surface 12-lead ECG was abnormal in 91% of patients with ACM who had a diagnosis of definitive ACM, according to the 2010 ITF criteria.[3] The present study was designed to investigate the relationship between electrocardiographic abnormalities and structural/functional remodeling of both ventricles on the basis of CE-CMR findings in patients with ACM. The main results were that electrocardiographic repolarization and depolarization abnormalities may predict the severity of RV dilatation/dysfunction and the coexistence of LV involvement, which are among the most important determinants of the disease phenotypic appearance and clinical outcome.[8,9]

Electrocardiographic Repolarization Abnormalities

Previous studies demonstrated that T waves in ACM typically become negative with the disease worsening and that negative T waves in the right precordial leads (V1-V3/V4) reflect the fibrofatty myocardial replacement, resulting in RV dilation and dysfunction.[15] Our study results confirm and extend these previous observations by demonstrating a relationship between the presence and extent of negative T waves and the degree of RV dilation and dysfunction, as evaluated by cine CMR sequences.

In previous studies, the extent of negative T waves across a 12-lead ECG was shown to predict the amount of RV electroanatomic scar, as evaluated by the voltage mapping at the CARTO (Biosense Webster, Inc) system.[16,17] However, the contributing role of LV scar involvement to left precordial TWI was not assessed because the map was limited to the RV. The present study allowed us to analyze the relationship between electrocardiographic repolarization abnormalities and the relative involvement of the RV, LV, or both, in terms of either end-diastolic volumes and ejection fraction by cine CMR sequences or LGE/myocardial scar by postcontrast sequences for tissue characterization. A major study result was that the extent of TWI toward the left precordial leads (V4-V6) and/or inferior leads was associated with a more severe RV dilation or dysfunction, whereas it did not predict

Table 4. Relationship Between Presence and Extent of Right Precordial TWI and CMR Parameters

Parameters	No TWI in Right Precordial Leads (n=18)	TWI in Right Precordial Leads Only (n=11)	TWI in Right Precordial+Left Precordial and/or Inferior Leads (n=50)	P Value
RV EDV, mL/m^2	92 (75–103)	94 (90–115)	117 (104–130)	<0.001
RV EF, %	57 (54–63)	49 (38–60)	41 (34–49)	<0.001
RV WMA, no. of segments	1 (0–2)	2 (1–3)	3 (2–4)	<0.001
RV dilatation*	6 (33)	9 (82)	46 (92)	<0.001
RV dysfunction (RV EF <45%)	1 (6)	4 (36)	32 (64)	<0.001
Displacement angle (α), °	40 (39–42)	36 (32–39)	52 (44–60)	0.02
Displacement ratio %LatD, %	60 (56–63)	52 (41–53)	97 (57–100)	<0.001
LV EDV, mL/m^2	92 (77–96)	89 (75–100)	82 (71–91)	0.192
LV EF, %	57 (49–64)	59 (52–63)	58 (48–62)	0.787
LV dilatation (≥90 mL/m^2)	11 (61)	5 (46)	17 (34)	0.131
LV dysfunction (≤50%)	7 (39)	1 (9)	14 (28)	0.221
RV LGE	9 (50)	5 (46)	41 (82)	0.007
LV LGE	13 (72)	7 (64)	37 (74)	0.786

Values are expressed as number (percentage) of patients or median (25th–75th percentile). α indicates cardiac apex angle; CMR, cardiac magnetic resonance; EDV, end-diastolic volume; EF, ejection fraction; %LatD, ratio of lateral displacement; LGE, late gadolinium enhancement; LV, left ventricular; RV, right ventricular; TWI, T-wave inversion; WMA, wall motion abnormality.
*According to International Task Force criteria, cutoff values were >100 mL/m^2 (men) and >90 mL/m^2 (women).

the involvement of the LV, either hemodynamic or structural, contrary to what one would expect.

The CE-CMR sequences also allowed us to find the plausible mechanism responsible for this finding. A previous electrocardiographic and vectorcardiographic correlation study reported that RV enlargement induces a backward displacement of the LV, with posterior dislocation of the LV electrical forces.[18] Using the technique previously reported by Brosnan et al,[14] we provided imaging evidence that the RV was displaced toward the axilla and a greater proportion of

Table 5. Relationship Between Low Voltages of QRS (<0.5 mV) in Limb Leads and CMR Parameters

Parameters	Low QRS Voltages		P Value
	No (n=63)	Yes (n=16)	
RV EDV, mL/m^2	109 (94–118)	105 (89–137)	0.864
RV EF, %	49 (38–56)	42 (30–60)	0.320
RV WMA, no. of segments	2 (1–4)	3 (2–4)	0.349
RV LGE	43 (68)	12 (75)	0.764
LV EDV, mL/m^2	85 (74–96)	86 (71–92)	0.403
LV EF, %	59 (51–64)	53 (46–59)	0.087
LV LGE	41 (65)	16 (100)	0.004
LV LGE, no. of segments	3 (2–7)	6 (5–9)	<0.001

Values are expressed as number (percentage) of patients or median (25th–75 percentile). CMR indicates cardiac magnetic resonance; EDV, end-diastolic volume; EF, ejection fraction; LGE, late gadolinium enhancement; LV, left ventricular; RV, right ventricular; WMA, wall motion abnormality.

the ventricle was positioned under the electrocardiographic leads placed more laterally, as a consequence of its dilatation. Hence, the traditional LV leads (V4-V6) explored the electrical activity of the RV rather than that of the LV. This accounts for the strong association between the extent of TWI toward the lateral precordial leads and the severity of RV dilatation (and dysfunction) leading to leftward displacement.

The electrogenesis of T-wave inversion in ACM and its relation to the severity of RV disease remain to be elucidated. On the basis of our findings, one can speculate that replacement of RV myocardium by fibrofatty tissue induces a RV remodeling, with both hemodynamic alterations leading to ventricular dilatation and dysfunction and electrical changes of transmural and/or regional activation and repolarization times. These electrophysiological changes may become critical enough to cause reversal of repolarization gradients and lead to T-wave inversion.

Electrocardiographic Depolarization Abnormalities

The electrocardiographic abnormalities of ACM resulting from delayed RV activation/conduction include incomplete (rarely complete) right bundle branch block, prolongation of right precordial QRS duration, delayed S-wave upstroke with a terminal activation delay of >55 ms, and postexcitation ε waves (ie, small-amplitude potentials occurring at the end of the QRS complex/beginning of the ST segment).[6,12] These electrocardiographic changes reflect areas of slow
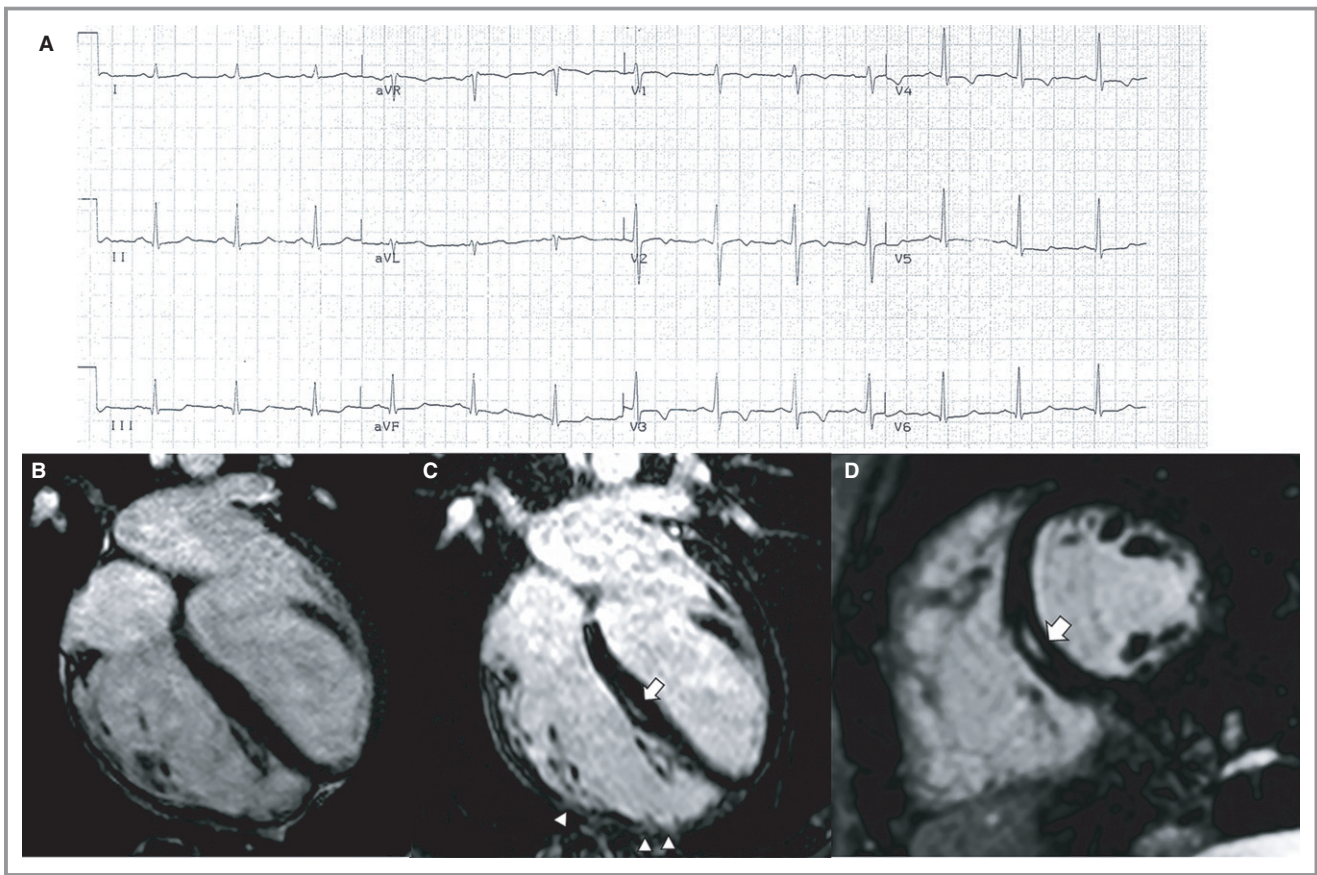
Figure 1. Electrocardiographic and contrast-enhanced cardiac magnetic resonance (CMR) findings of a representative case of right-dominant (classic) arrhythmogenic cardiomyopathy variant. **A**, Basal ECG showing T-wave inversion in right precordial leads (V1-V4). **B**, End-diastolic frame of cine CMR sequence in long-axis 4-chamber view showing a dilated right ventricle (end diastolic volume, 127 mL/m^2) with a severely reduced ejection fraction (25%). The postcontrast orthogonal images in long-axis (**C**) and short-axis (**D**) views show late gadolinium enhancement as midwall stria in the midseptum (white arrow). In **C**, late gadolinium enhancement is also visible in the anterolateral, mid, and apical regions of the right ventricular wall, with segmental transmural involvement (white arrowheads) associated with regional dyskinesia (not shown).

intraventricular conduction, in which the underlying substrate consists of regions of surviving myocardium interspersed with fatty and fibrous tissue. These can cause fragmentation of the electric activation of the ventricular myocardium and predispose to reentrant ventricular arrhythmias. Experimental studies have showed that susceptible desmosomal-gene carriers may harbor arrhythmogenic mechanisms at a molecular and cellular level because of a cross talk between altered desmosomes and both voltage-gated sodium-channel and gap junction proteins.[19–21] Loss of expression of desmosomal proteins may induce electrical ventricular instability by a concomitant sodium channel dysfunction with current reduction, as a consequence of the interaction of these molecules at the intercalated discs. These findings have raised concerns that desmosomal-gene mutation carriers may experience life-threatening ventricular arrhythmias before fibrofatty myocardial replacement, structural/functional ventricular abnormalities develop, and sudden cardiac death may occur during the so-called concealed phase of the disease. However, clinical outcome studies did not support this hypothesis, showing that phenotypic expression is a prerequisite for malignant arrhythmic events and sudden cardiac death in ACM.[22,23]

Among depolarization/activation abnormalities, in our study, abnormal prolongation of TAD (>55 ms) was the most important electrocardiographic predictor of RV dilatation and dysfunction. An abnormal TAD was observed in 40% of our study patients and was significantly associated with a worse RV disease, characterized by greater cavity dimension and more reduced systolic function. The TAD interval, which, according to the original definition, extends from the nadir of the S wave to the end of all depolarization deflections, is an expression of the global RV activation time, including other depolarization abnormalities, such as prolonged QRS duration, delayed and fractionated S-wave upstroke, and ε waves.[13]

The ε waves are an uncommon finding in patients with advanced disease and are usually associated with the positivity of other diagnostic criteria. In the present study,
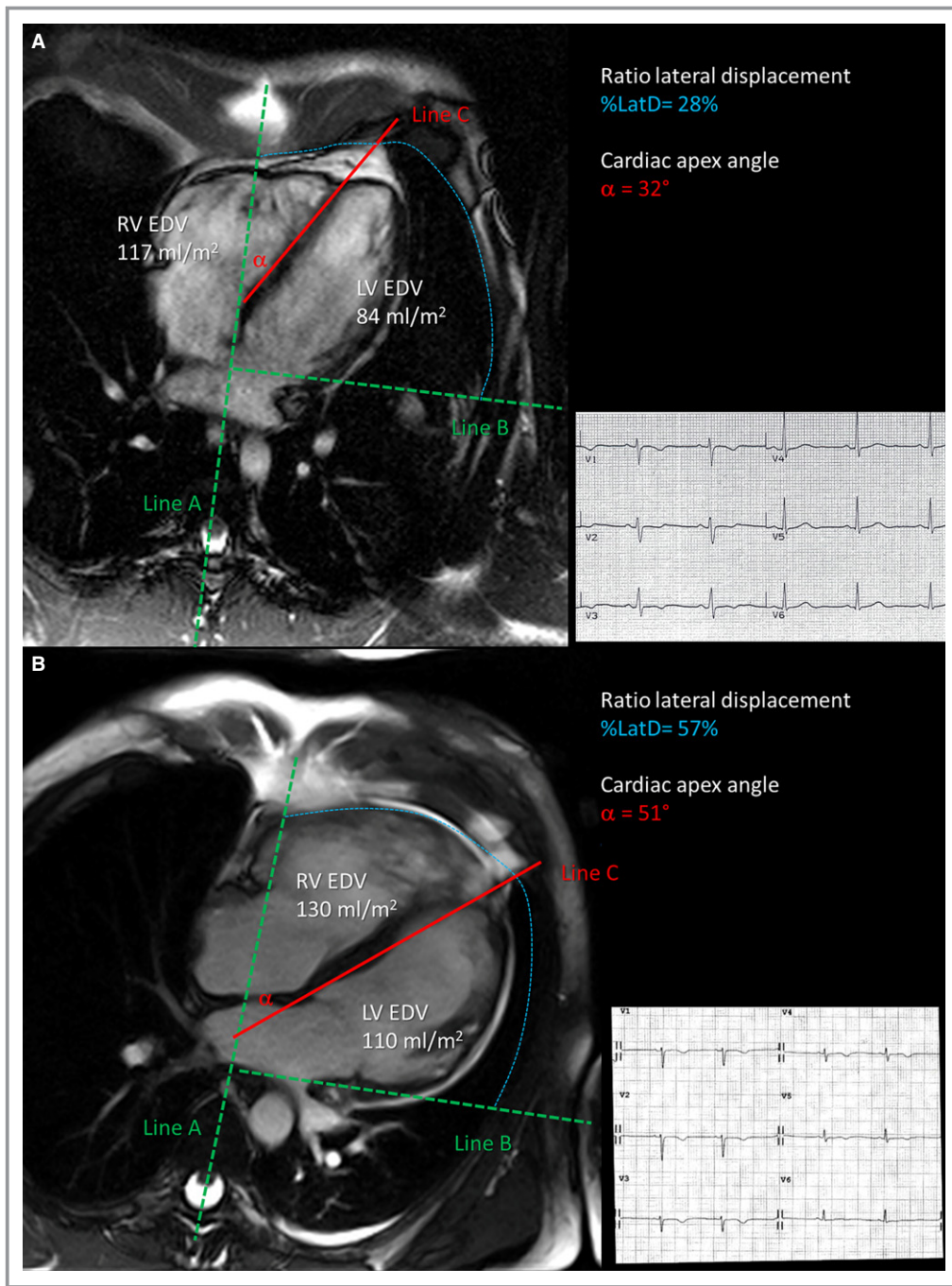
Figure 2. Relationship between extent of T-wave inversion across precordial leads and right ventricular dilatation. End-diastolic frame of cine cardiac magnetic resonance sequences in long-axis 4-chamber view, showing measurement of the degree of right ventricular (RV) dilatation and displacement across the precordial plane in 2 study patients. In patient A with T-wave inversion confined to right precordial leads, a mild dilatation of the RV (117 mL/m^2) does not induce displacement of the cardiac apex toward the left axilla (cardiac apex angle [α]=32°). In patient B with T-wave inversion extending to the left precordial leads, a severely dilated RV (130 mL/m^2) leads to displacement of the cardiac apex toward the lateral precordium. EDV indicates end-diastolic volume; %LatD, ratio of lateral displacement; LV, left ventricular.

postexcitation ε waves were found in only 16% of patients, and any statistical association with structural or functional CE-CMR abnormalities was not demonstrable.

The finding that depolarization abnormalities were unrelated to LV involvement was expected, given that all these electrocardiographic depolarization parameters are confined
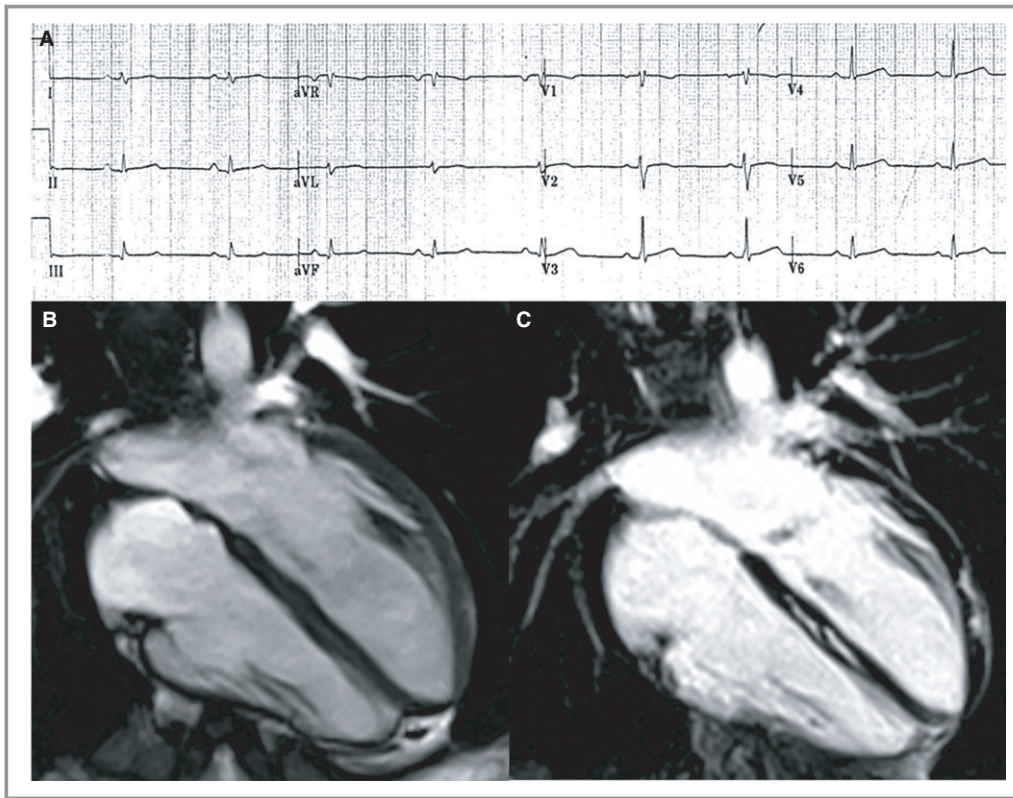
Figure 3. Electrocardiographic and contrast-enhanced cardiac magnetic resonance (CMR) findings of a representative case of left-dominant arrhythmogenic cardiomyopathy variant in a patient with a desmoplakin-gene mutation and a history of sustained ventricular tachycardia. **A**, Basal ECG showing low QRS voltages (<0.5 mV) in limb leads. **B**, End-diastolic frame of cine CMR sequence in long-axis 4-chamber view showing normal cavity size and function of both ventricles. **C**, Postcontrast image showing myocardial fibrosis in the form of stria of late gadolinium enhancement in the epicardium of the left ventricular lateral wall (arrowheads) and midmural layer of the interventricular septum (arrows).

to right precordial leads and their alterations indicate a right intraventricular conduction defect.

Low QRS Voltages in Limb Leads

The electrocardiographic pattern of low QRS voltages in the limb leads with normal precordial amplitudes is the result of conditions that either alter voltage transmission or impair voltage generation from the myocardium to the skin electrodes, such as pericardial or large pleural effusion, infiltrative cardiomyopathy, and obesity.[24] Several studies reported anecdotal evidence that low QRS voltages in limb leads may reflect the presence of a segmental LV scar/ LGE, which can be evidenced by CE-CMR.[25–27] Actually, CE-CMR has emerged as the imaging test that allows the "in vivo" detection and the characterization of LV involvement in ACM, in terms of dilatation and systolic dysfunction assessed by cine CMR sequences and/or fibrofatty scar detected by postcontrast CMR sequences.[7] On the basis of the presence and extent of the coexistent LV involvement,

the spectrum of ACM phenotypes has broadened to include "biventricular" and "left-dominant" variants, in addition to the classic "right-dominant" form.[1,2,4,5,8] The LV lesions consist of fibrofatty myocardial replacement, which may affect the free wall, the interventricular septum, or both, either diffusely or regionally, with a predilection for the posterolateral regions. Like RV lesions, the wave front of fibrofatty myocardial replacement in the LV progresses from the epicardium to the endocardium, with scar tissue typically confined to subepicardial/midmural layers. The presence of LV involvement was originally considered a sign of advanced disease, being an end-stage manifestation and leading ultimately to biventricular pump failure. More recent genotype-phenotype correlation studies have shown early and greater LV involvement related to some genetic defects, such as desmoplakin-gene mutations.[28]

The present study extended previous observations[25–27] by showing that the electrocardiographic pattern of low QRS voltages may predict LV involvement in the context of ACM with a specificity of 100%, although its sensitivity did not

exceed 30%. The mechanism involved in the reduction of QRS voltages reasonably consists of the decrease of LV myocardial mass, which mostly accounts for the generation of the electrical activity causing the depolarization current responsible for the QRS complex. Why it mainly affects the limb leads remains to be elucidated. The low sensitivity of low QRS voltages may be explained by a dose–effect relationship between myocardial replacement by fibrofatty scar and reduction in QRS amplitudes in limb leads. This is in keeping with the significantly higher number of LV segments affected by LGE in patients with than in those without low QRS voltages on the ECG.

Our results indicate that low QRS voltages are a useful diagnostic marker of the "biventricular" variant of ACM because it may predict the coexistence of LV involvement by significant fibrofatty myocardial replacement, with important implications on clinical evaluation and monitoring over follow-up of the LV systolic function, which is a crucial parameter of outcome.[29] Moreover, there is growing evidence that an LV scar "per se" may increase the risk of life-threatening ventricular arrhythmias and sudden cardiac death, even in the absence of significant systolic dysfunction.[30]

Conclusion

The study results indicate that electrocardiography has the potential to predict the ACM phenotype, with particular reference to the severity of RV disease and LV involvement, which are among the most important clinical determinants of the disease outcome. Specifically, the extent of TWI toward left precordial and inferior leads and prolonged TAD predicted higher RV dilation and lower RV ejection fraction, whereas low QRS voltages in limb leads predicted the presence of LV LGE/ scar. These findings support the concept that routine electrocardiography in ACM provides both diagnostic and prognostic information. According to the 2010 ITF diagnostic criteria for ACM, the electrocardiographic pattern of TWI in V4, V5, or V6 is the only proposed electrocardiographic criterion for LV involvement. Our study results suggest considering the electrocardiographic pattern of low QRS voltages in limb leads, which was shown to be a more accurate predictor of LV involvement.

Disclosures

None.

Sources of Funding

References

1. Corrado D, Link MS, Calkins H. Arrhythmogenic right ventricular cardiomyopathy. N Engl J Med. 2017;376:61–62.
2. Corrado D, Basso C, Judge DP. Arrhythmogenic cardiomyopathy. Circ Res. 2017;121:784–802.
3. Marcus FI, McKenna WJ, Sherrill D, Basso C, Bauce B, Bluemke DA, Calkins H, Corrado D, Cox MG, Daubert JP, Fontaine G, Gear K, Hauer R, Nava A, Picard MH, Protonotarios N, Saffitz JE, Sanborn DM, Steinberg JS, Tandri H, Thiene G, Towbin JA, Tsatsopoulou A, Wichter T, Zareba W. Diagnosis of arrhythmogenic right ventricular cardiomyopathy/dysplasia. Circulation. 2010;121:1533–1541.
4. Sen-Chowdhry S, Syrris P, Prasad SK, Hughes SE, Merrifield R, Ward D, Pennell DJ, McKenna WJ. Left-dominant arrhythmogenic cardiomyopathy: an under-recognized clinical entity. J Am Coll Cardiol. 2008;52:2175–2187.
5. Marra MP, Leoni L, Bauce B, Corbetti F, Zorzi A, Migliore F, Silvano M, Rigato I, Tona F, Tarantini G, Cacciavillani L, Basso C, Buja G, Thiene G, Iliceto S, Corrado D. Imaging study of ventricular scar in arrhythmogenic right ventricular cardiomyopathy: comparison of 3D standard electroanatomical voltage mapping and contrast-enhanced cardiac magnetic resonance. Circ Arrhythm Electrophysiol. 2012;5:91–100.
6. Nasir K, Bomma C, Tandri H, Roguin A, Dalal D, Prakasa K, Tichnell C, James C, Spevak PJ, Marcus F, Calkins H. Electrocardiographic features of arrhythmogenic right ventricular dysplasia/cardiomyopathy according to disease severity: a need to broaden diagnostic criteria. Circulation. 2004;110:1527–1534.
7. Pontone G, Di Bella G, Silvia C, Maestrini V, Festa P, Ait-Ali L, Masci PG, Monti L, di Giovine G, De Lazzari M, Cipriani A, Guaricci AI, Dellegrottaglie S, Pepe A, Marra MP, Aquaro GD. Clinical recommendations of cardiac magnetic resonance, part II: inflammatory and congenital heart disease, cardiomyopathies and cardiac tumors: a position paper of the working group "Applicazioni della Risonanza Magnetica" of the Italian Society of Cardiology. J Cardiovasc Med. 2017;18:209–222.
8. Perazzolo Marra M, Rizzo S, Bauce B, De Lazzari M, Pilichou K, Corrado D, Thiene G, Iliceto S, Basso C. Arrhythmogenic right ventricular cardiomyopathy: contribution of cardiac magnetic resonance imaging to the diagnosis. Herz. 2015;40:600–606.
9. Corrado D, Wichter T, Link MS, Hauer RN, Marchlinski FE, Anastasakis A, Bauce B, Basso C, Brunckhorst C, Tsatsopoulou A, Tandri H, Paul M, Schmied C, Pelliccia A, Duru F, Protonotarios N, Estes NM III, McKenna WJ, Thiene G, Marcus FI, Calkins H. Treatment of arrhythmogenic right ventricular cardiomyopathy/dysplasia: an international task force consensus statement. Circulation. 2015;132:441–453.
10. Calkins H, Corrado D, Marcus F. Risk stratification in arrhythmogenic right ventricular cardiomyopathy. Circulation. 2017;136:2068–2082.
11. Migliore F, Zorzi A, Michieli P, Perazzolo Marra M, Siciliano M, Rigato I, Bauce B, Basso C, Toazza D, Schiavon M, Iliceto S, Thiene G, Corrado D. Prevalence of cardiomyopathy in Italian asymptomatic children with electrocardiographic T-wave inversion at preparticipation screening. Circulation. 2012;125:529–538.
12. Cox MG, Nelen MR, Wilde AA, Wiesfeld AC, van der Smagt JJ, Loh P, Cramer MJ, Doevendans PA, van Tintelen JP, de Bakker JM, Hauer RN. Activation delay and VT parameters in arrhythmogenic right ventricular dysplasia/cardiomyopathy: toward improvement of diagnostic ECG criteria. J Cardiovasc Electrophysiol. 2008;19:775–781.
13. Fontaine G, Umemura J, Di Donna P, Tsezana R, Cannat JJ, Frank R. Duration of QRS complexes in arrhythmogenic right ventricular dysplasia: a new non-invasive diagnostic marker. Ann Cardiol Angeiol (Paris). 1993;42:399–405.
14. Brosnan MJ, Claessen G, Heidbuchel H, Prior DL, La Gerche A. Right precordial T-wave inversion in healthy endurance athletes can be explained by lateral displacement of the cardiac apex. JACC Clin Electrophysiol. 2015;1:84–91.
15. Marcus FI. Prevalence of T-wave inversion beyond V1 in young normal individuals and usefulness for the diagnosis of arrhythmogenic right ventricular cardiomyopathy/dysplasia. Am J Cardiol. 2005;95:1070–1071.
16. Tanawuttiwat T, Te Riele AS, Philips B, James CA, Murray B, Tichnell C, Sawant AC, Calkins H, Tandri H. Electroanatomic correlates of depolarization abnormalities in arrhythmogenic right ventricular dysplasia/cardiomyopathy. J Cardiovasc Electrophysiol. 2016;27:443–452.
17. Zorzi A, Migliore F, Elmaghawry M, Silvano M, Marra MP, Niero A, Nguyen K, Rigato I, Bauce B, Basso C, Thiene G, Iliceto S, Corrado D. Electrocardiographic predictors of electroanatomic scar size in arrhythmogenic right ventricular cardiomyopathy: implications for arrhythmic risk stratification. J Cardiovasc Electrophysiol. 2013;24:1321–1327.
18. Nava A, Canciani B, Buja G, Martini B, Daliento L, Scognamiglio R, Thiene G. Electrovectorcardiographic study of negative T waves on precordial leads in

arrhythmogenic right ventricular dysplasia: relationship with right ventricular volumes. *J Electrocardiol*. 1988;21:239–245.

19. Rizzo S, Lodder EM, Verkerk AO, Wolswinkel R, Beekman L, Pilichou K, Basso C, Remme CA, Thiene G, Bezzina CR. Intercalated disc abnormalities, reduced Na(+) current density, and conduction slowing in desmoglein-2 mutant mice prior to cardiomyopathic changes. *Cardiovasc Res*. 2012;95:409–418.

20. Sato PY, Musa H, Coombs W, Guerrero-Serna G, Patino GA, Taffet SM, Isom LL, Delmar M. Loss of plakophilin-2 expression leads to decreased sodium current and slower conduction velocity in cultured cardiac myocytes. *Circ Res*. 2009;105:523–536.

21. Kaplan SR, Gard JJ, Protonotarios N, Tsatsopoulou A, Spiliopoulou C, Anastasakis A, Squarcioni CP, McKenna WJ, Thiene G, Basso C, Brousse N, Fontaine G, Saffitz JE. Remodeling of myocyte gap junctions in arrhythmogenic right ventricular cardiomyopathy due to a deletion in plakoglobin (Naxos disease). *Heart Rhythm*. 2004;1:3–11.

22. Te Riele AS, Bhonsale A, James CA, Rastegar N, Murray B, Burt JR, Tichnell C, Madhavan S, Judge DP, Bluemke DA, Zimmerman SL, Kamel IR, Calkins H, Tandri H. Incremental value of cardiac magnetic resonance imaging in arrhythmic risk stratification of arrhythmogenic right ventricular dysplasia/ cardiomyopathy-associated desmosomal mutation carriers. *J Am Coll Cardiol*. 2013;62:1761–1769.

23. Zorzi A, Rigato I, Pilichou K, Perazzolo Marra M, Migliore F, Mazzotti E, Gregori D, Thiene G, Daliento L, Iliceto S, Rampazzo A, Basso C, Bauce B, Corrado D. Phenotypic expression is a prerequisite for malignant arrhythmic events and sudden cardiac death in arrhythmogenic right ventricular cardiomyopathy. *Europace*. 2016;18:1086–1094.

24. Chinitz JS, Cooper JM, Verdino RJ. Electrocardiogram voltage discordance: interpretation of low QRS voltage only in the limb leads. *J Electrocardiol*. 2008;41:281–286.

25. Gallo C, Blandino A, Giustetto C, Anselmino M, Castagno D, Richiardi E, Gaita F. Arrhythmogenic right ventricular cardiomyopathy: ECG progression over time and correlation with long-term follow-up. *J Cardiovasc Med*. 2016;17:418–424.

26. Gaido L, Battaglia A, Matta M, Giustetto C, Frea S, Imazio M, Richiardi E, Garberoglio L, Gaita F. Phenotypic expression of ARVC: how 12 lead ECG can predict left or right ventricle involvement: a familiar case series and a review of literature. *Int J Cardiol*. 2017;236:328–334.

27. Steriotis AK, Bauce B, Daliento L, Rigato I, Mazzotti E, Folino AF, Marra MP, Brugnaro L, Nava A. Electrocardiographic pattern in arrhythmogenic right ventricular cardiomyopathy. *Am J Cardiol*. 2009;103:1302–1308.

28. Norman M, Simpson M, Mogensen J, Shaw A, Hughes S, Syrris P, Sen-Chowdhry S, Rowland E, Crosby A, McKenna WJ. Novel mutation in desmoplakin causes arrhythmogenic left ventricular cardiomyopathy. *Circulation*. 2005;112:636–642.

29. Zorzi A, Rigato I, Bauce B, Pilichou K, Basso C, Thiene G, Iliceto S, Corrado D. Arrhythmogenic right ventricular cardiomyopathy: risk stratification and indications for defibrillator therapy. *Curr Cardiol Rep*. 2016;18:57.

30. Zorzi A, Perazzolo Marra M, Rigato I, De Lazzari M, Susana A, Niero A, Pilichou K, Migliore F, Rizzo S, Giorgi B, De Conti G, Sarto P, Serratosa L, Patrizi G, De Maria E, Pelliccia A, Basso C, Schiavon M, Bauce B, Iliceto S, Thiene G, Corrado D. Nonischemic left ventricular scar as a substrate of life-threatening ventricular arrhythmias and sudden cardiac death in competitive athletes. *Circ Arrhythm Electrophysiol*. 2016;9:e004229.